*Korean J. Chem. Eng.*, 39(11), 2916-2924 (2022)
DOI: 10.1007/s11814-022-1222-0

pISSN: 0256-1115
eISSN: 1975-7220

# Development of real time responding hydrogen fueling protocol and its risk assessment

**Chung Keun Chae*, Byung Heung Park**, Seung Kyu Kang***, Jae-Ou Choi****, Jin Hyung Park*****, Wangyun Won******, and Yeonsoo Kim*******,†**

*Mirae EHS-code Research Institute, Seoul 14353, Korea
**Department of Chemical and Biological Engineering, Korea National University of Transportation, 50 Daehak-ro, Chungju-si, Chungcheongbuk-do 27469, Korea
***Korea Gas Safety Corporation, Eumseong 27738, Korea
****Pohang Institute of Science and Technology, Pohang 37673, Korea
*****Safety Health Convergence Engineering Department, Soongsil University, 369 Sangdo-ro, Dongjak-gu, Seoul 06978, Korea
******Department of Chemical Engineering (Integrated Engineering), Kyung Hee University, 1732 Deogyeong-daero, Giheung-gu, Yongin-si, Gyeonggi-do 17104, Korea
*******Department of Chemical Engineering, Kwangwoon University, 20 Kwangwoon-ro, Nowon-gu, Seoul 01897, Korea
(*Received 17 March 2022 • Revised 21 June 2022 • Accepted 3 July 2022*)

**Abstract**−Existing hydrogen fueling protocols (HFP), such as SAE J2601, have limitations in low efficiency and limited applicability for various vehicle types. They use lookup tables or formulas constructed by simulation and do not calculate the optimal fueling strategy in real-time. To address this issue, we proposed a real-time responding HFP (RTR-HFP) in our previous study and further improved the RTR-HFP in this study. We introduced a tuning parameter to transform the simplified model from the extreme case to the real case, and we can determine a less conservative pressure ramp rate (PRR) by RTR-HFP in real-time. In addition, to avoid unstable fueling issues when the storage system pressure is too low, we integrated the RTR-HFP with the existing table-based strategy and determined the best PRR while restricting the upper bound on PRR. Furthermore, we performed a risk assessment of the fueling system and found a solution to ensure the safety integrity level in the control system.

Keywords: Hydrogen Fueling Protocol, Hydrogen Refueling Station, Compressed Hydrogen Storage System, Average Pressure Ramp Rate, Real-time Responding HFP

## INTRODUCTION

Hydrogen fuel cell vehicles are eco-friendly and have high thermal efficiency. To realize increased adoption of hydrogen fuel cell vehicles and to ensure competitiveness compared with other existing fuel cell vehicles, it is important to ensure safety and fast charging [1]. However, it is difficult to rapidly charge and completely fill hydrogen fuel cell vehicles, because a large amount of heat is generated owing to compression when compressed hydrogen enters the tank [2-4]. To control the issue, the hydrogen fuel protocol (HFP) was developed. The HFPs currently used across the world are included in SAE J2601 and JPEC-S 0003 [5,6].

Traditional HFPs can be divided into table-based HFPs (TB-HFP) and MC formula-based HFPs (MC-HFP). TB-HFPs select the pressure ramp rate (PRR) and target pressure from lookup tables depending on the ambient temperature and the tank pressure; whereas MC-HFPs use formulas to determine the target pressure and the PRR in real time based on the supply temperature and pressure of compressed hydrogen at dispensers, ambient temperature, and hydrogen pressure in the compressed hydrogen storage system (CHSS) [7,8]. Traditional HFPs assume two extreme-case scenarios called hot and cold cases. All fueling conditions are considered to be between the two extremes. In addition, non-communication with the vehicle tank sensors is basically assumed; thus, these HFPs provide inefficient PRRs, resulting in slow fueling.

In our previous work [9], we developed a rigorous thermodynamic model (RTM); the RTM was then simplified into a simple thermodynamic model (STM), ignoring the heat exchange with the ambient environment in the fueling line and the vehicle tank. The RTM was validated with the experimental data in [1] and showed errors smaller than 3% for the maximum values of temperature, pressure, and mass flow rate. However, there were deviations in the temperature when the simulation results by STM were compared with those of RTM, whereas other variables such as tank pressure and state of charge (SOC) were almost the same for both cases. In addition, we proposed a new HFP in the communication setting; the effectiveness of which was verified using the RTM as a virtual plant. For every sampling time, the current temperature and pressure in the tank were given, and safety-related variables such as temperature and pressure in the tank and the hydrogen mass flow

†To whom correspondence should be addressed.
E-mail: kimy3@kw.ac.kr

rate were predicted for a given PRR until the SOC reached 100%. If the maximum values of the safety-related variables did not exceed the constraints, then the PRR was increased, and the prediction repeated. If, on the other hand, the maximum values of the safety-related variables exceeded the constraints, the PRR was reduced. This strategy allowed us to implement a safe PRR to fill the tank quickly. In our previous HFP, the control performance was validated using the parameters of the hot case of SAE J2601.

In this study, we improved the applicability of our previous HFP and conducted a risk assessment for its real implementation. First, we improved the STM by introducing a hypothetical fueling line inner diameter ($d_{FL}$). This diameter was first calibrated to show the same results written in SAE J2601 under hot cases with TB-HFP, and then we calibrated $d_{FL}$ for each real case by a leak pressure test, resulting in a less conservative application of the HFP. This is a similar idea to Ref. [10], where the valve parameter was used as a calibration parameter. With the improved STM, we can extend our previously proposed HFP to real-world scenarios. Second, to ensure operability under initial low-pressure conditions, we suggest using a fixed APRR from the TB-HFP during early fueling when the pressure is low in the CHSS. To improve safety, we set the upper limit of the PRR based on the remaining fueling time and volume to prevent over-fueling. Finally, we conduct a risk assessment to determine the safety integrity level (SIL) for real implementation.

The remainder of this paper is organized as follows. Section 2 describes the existing and improved STM. The performance of the RTR-HFP is evaluated in terms of stability, safety, versatility, and functional safety in Sections 3 and 4.

## IMPROVEMENT OF SIMPLIFIED THERMODYNAMIC MODEL (STM)

### 1. The Previous STM

We first summarize the STM developed in our previous work [9] for the completeness of the paper, and then explain the improvement in the next subsection. The STM is used to predict the pressure and temperature of the compressed hydrogen in the CHSS when the current pressure and temperature measurements in both the CHSS and breakaway are given and the PRR is determined. Depending on the selected value of the PRR, the pressure and temperature in the CHSS, and the hydrogen mass flow rate change with time.

At time step t, the breakaway pressure during the future horizon can be calculated from the current measurement and the determined PRR using the following equation:

$$P_{ba}(t+1) = P_{ba}(t) + (PRR(t) \times \Delta T_s). \tag{1}$$

Here, $P_{ba}$ denotes the breakaway pressure and $\Delta T_s$ is the sampling time.

The fueling line consists of a tube with a small inner diameter and other components, which causes a large pressure drop when compressed hydrogen is fueled. The pressure drop can be approximated using the pressure loss factor $K_{FL}$ as follows [11-13]:

$$\Delta P_{FL}(t) = P_{ba}(t) - P_{tk}(t) = K_{FL}\frac{(\dot{m}_{FL})^2}{\rho_{FL}} \tag{2}$$

In the previous STM, $K_{FL}$ was taken to be the value of the hot case in SAE J2601, which is an extreme case. In this study, the pressure loss factor was adjusted by calibrating the $d_{FL}$ for various sizes of tanks under the hot case condition, and then, for real case conditions, we propose an online calibration strategy. This will be discussed in the next subsection. At time step t, the pressure in the tank was also measured to calculate the hydrogen mass flow rate of the fueling line $\dot{m}_{FL}$ from Eq. (2), as follows:

$$\dot{m}_{FL} = \sqrt{\frac{\rho_{FL}(P_{ba} - P_{tk})}{K_{FL}}} \tag{3}$$

Here, $P_{tk}$ denotes the tank pressure. $\rho_{FL}$ is the average density of the gas in the fueling line, and it is calculated using the density function from Eq. J98 in Section J.3.5, SAE J2601 [5]. The density function is denoted by $f_\rho$; its first argument is pressure, and the second argument is temperature.

$$\rho_{FL} = f_\rho\left(\frac{P_{ba}+P_{tk}}{2}, \frac{T_{ba}+T_{tk}}{2}\right) \tag{4}$$

The final mass flow rate to each tank, $\dot{m}_{ti}$, is calculated by dividing $\dot{m}_{FL}$ by the number of tanks, as described in Eq. (5).

$$\dot{m}_{ti} = \frac{\dot{m}_{FL}}{N_{tk}} \tag{5}$$

Here, $N_{tk}$ denotes the number of tanks.

The temperature in the CHSS is affected by the stagnation enthalpy of the gas entering the vehicle tank when the pressure drop from the friction in the fueling line is negligible [14,15]:

$$h_{sg,\,ti} = h_{ti} + \frac{v_{ti}^2}{2} = h_{ba} + \frac{v_{ba}^2}{2} \tag{6}$$

Here, the enthalpy at the tank inlet and breakaway are denoted as $h_{ti}$ and $h_{ba}$, respectively. The linear velocities at the tank and breakaway are represented by $v_{ti}$ and $v_{ba}$, respectively. The correlation of enthalpy with pressure and temperature is given by Eq. J95 in Section J.3.1. of SAE J2601 [5]. Denoting the enthalpy correlation of hydrogen gas as $f_h(P, T)$, $h_{ti}$ is calculated as $f_h(P_{tk}, T_{tk})$ and $h_{ba}$ is calculated as $f_h(P_{ba}, T_{ba})$. Linear velocity $v_{ba}$ is calculated as follows:

$$v_{ba} = \frac{\dot{m}_{FL}}{N_{tk}}\frac{4}{\pi d_{ba}^2 \rho_{FL}} \tag{7}$$

$$\dot{m}_{FL} = \sqrt{\frac{\rho_{FL}(P_{ba} - P_{tk})}{K_{FL}}} \tag{8}$$

From Eq. (6) and the enthalpy correlation $f_h$, the stagnation enthalpy of the gas entering the vehicle tank is calculated as follows:

$$h_{sg,\,ti} = f_h(P_{ba}, T_{ba}) + \frac{v_{ba}^2}{2} = f_h(P_{ba}, T_{ba}) + \frac{8\Delta P_{FL}}{K_{FL}\rho_{FL}(\pi d_{ba}^2 N_{tk})^2} \tag{9}$$

Here the second equality is obtained by Eqs. (3) and (5) and $\Delta P_{FL} = P_{ba} - P_{tk}$.

The energy balance for temperature is constructed as Eq. (10), which is simplified into a discretized form as Eq. (11).

$$\frac{d(m_{tk}C_v T_{tk})}{dt} = h_{sg,\,ti}\dot{m}_{ti} - Q_{tk} \tag{10}$$

$$T_{tk}(t)=\frac{(h_{sg,ti}(t)\dot{m}_{ti}(t)-Q_{tk})\Delta T_s+(C_v(t-1)m_{tk}(t-1)T_{tk}(t-1))}{C_v(t-1)(m_{tk}(t-1)+\dot{m}_{ti}(t)\Delta T_s)} \quad (11)$$

Here, $C_v$ is the specific heat capacity at constant volume that is dependent on pressure and temperature. The correlation is also referred to in Eq. J99 in Section J.3.6. of SAE J2601. We assume that the value of $C_v$ can be regarded constant during the sampling time. Thus, to calculate the hydrogen temperature in the tank at time step t, $C_v(t)$ was assumed to be equal to $C_v(t-1)$. $Q_{tk}$ denotes the heat exchange between the fueling line and ambient environment, and it is assumed to be negligible.

Based on the calculated results, the tank pressure can be calculated as follows [16-18]:

$$Z_{tk}=1+\sum_{j=1}^{9}100a_j(T_{tk})^{-b_j}(P_{tk})^{c_j} \quad (12)$$

$$P_{tk}=Z_{tk}\rho_{tk}RT_{tk} \quad (13)$$

where $a_j$, $b_j$, and $c_j$ used in Eq. (12) were obtained from a previous study [18].

## 2. The Improved STM

The STM was improved to predict the CHSS temperature better than the previous STM. We first introduced a hypothetical fueling line inner diameter $d_{FL}$ to describe the increase of the tank temperature when the hydrogen enters the tank. In addition, the pressure drops from the dispenser to break-away and from the break-away to the tank were not considered separately because, in the real system, we cannot measure the pressure drops separately. Accordingly, the sum of pressure drop was considered with one parameter $d_{FL}$ and with the assumption that the inner diameter of the fueling line is constant.

Thus, the total energy, $h_{sg,ti}$, of Eq. (6) is calculated as follows:

$$h_{sg,ti}=h_{ba}+\left(\frac{v_{ba}^2}{2}\right) \text{ with } v_{ba}=\frac{\dot{m}}{\rho_{FL}A_{ba}}=\frac{4\dot{m}}{\rho_{FL}\pi d_{FL}^2} \quad (14)$$

Furthermore, $K_{FL}$ can be represented as

$$K_{FL}=\frac{\rho_{FL}\Delta P}{\dot{m}^2}=\frac{16\rho_{FL}\Delta P}{\rho_{FL}^2 v_{ba}^2\pi^2 d_{FL}^4} \quad (15)$$

The lookup table in SAE J2601 applied to the TB-HFP was prepared for tank capacity (2, 4, 7, 10 kg), supply gas temperature (T20, T30, T40), and an outdoor air temperature range (−40 to +50 °C). The PRR in TB-HFP of SAE J2601 was determined to ensure that the maximum temperature of the CHSS did not exceed 85 °C when the fueling was conducted in the hot case conditions. As the fueling proceeds, the CHSS temperature gradually increases to 85 °C at a full charge of 100% SOC. To match the condition, we fit the reference values of $d_{FL,ref}$ and the values are shown in Table 1. Although $d_{FL,ref}$ varies depending on the supply gas temperature, the difference is not substantial.

**Table 1. Calibration results of $d_{FL,ref}$**

| Tank capacity (kg) | $d_{FL,ref}$ (m) |
|---|---|
| 2 | 0.000682 |
| 4 | 0.000985 |
| 7 | 0.00133 |
| 10 | 0.00149 |

## 3. Conversion Strategy for Real Case

Parameters in the STM hot case led to a $T_{tk}$ of 85 °C and 95% SOC, whereas parameters in the real case led to different values of $T_{tk}$ and SOC under the same PRR condition determined by TB-HFP.

From Eq. (15), the following correlation is obtained:

$$d_{FL}\propto\left(\frac{1}{K_{FL}}\right)^{0.25} \quad (16)$$

We get the following equation, which gives $d_{FL}$ for the real case:

$$d_{FL}=d_{FL,ref}\left(\frac{K_{FL,ref}}{K_{FL}}\right)^{0.25} \quad (17)$$

Before the main fueling starts, the initial pressure pulse stage is conducted to check the leakage along the fueling line. During this pulse test, we can check the pressure loss coefficient for the real case, $K_{FL}$. Then, the $d_{FL}$ is calculated from Eq. (17) and the STM with these parameters for the real case is used with RTR-HFP.

# PERFORMANCE OF RTR-HFP

## 1. Stability of RTR-HFP

As shown in Fig. 1, the RTR-HFP uses thermodynamic data collected in real time, calculates the PRR based on real-time simula-

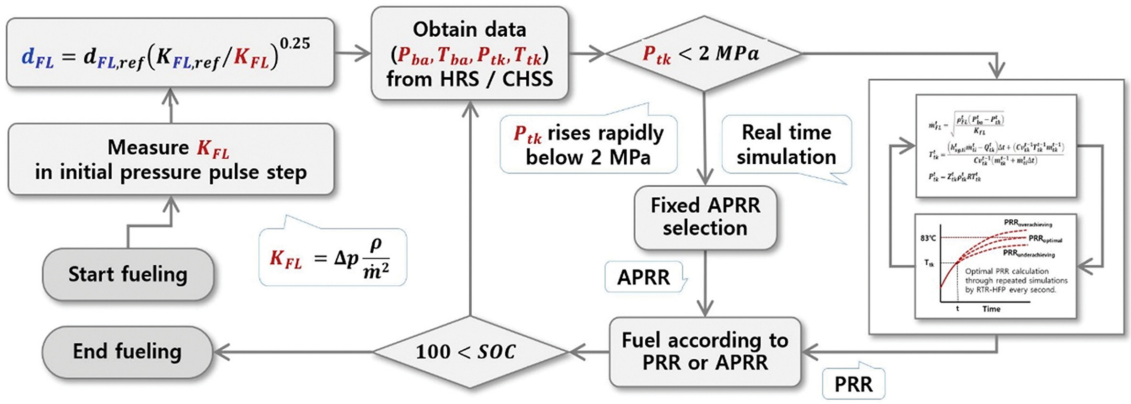


**Fig. 1. Concept of RTR-HFP logic.**

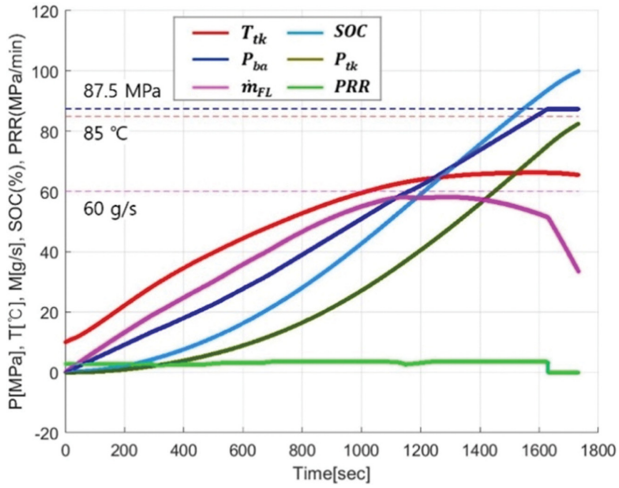


**Fig. 2. Extreme condition control ability of RTR-HFP; nominal working pressure of 70 MPa, $V_{tk}$ of 1,740 L (ten 174 L tanks), initial tank pressure of 0 MPa, and $T_{amb}$ of 10 °C.**

tion, applies it to the fueling process, and controls the process. In the early stage of the fueling process, when the volume of gas in the CHSS is low, the injected gas increases the temperature of the gas in the CHSS. The higher the supply gas temperature and outside air temperature, the more severe the phenomenon. During the development of the RTR-HFP based on simulations, the PRR calculation took too long, or the PRR changed rapidly after the calculation, which rendered it impossible to control. We used the pre-calculated APRR in the TB-HFP to overcome these issues and not the PRR in real time, if the pressure of the gas in the CHSS was less than or equal to 2 MPa. Hence, the operability issue was resolved, while the benefits of the RTR-HFP were significantly improved. Applying a fixed APRR to the early stage of fueling might cause a slight decrease in the efficiency of the fueling protocol (delay in fueling time). Because the initial pressure of the CHSS was less than 2 MPa in very few cases, the decrease in efficiency was small. An analysis of 37,000 cases fueled by MC-HFP in the US showed that the initial pressure of the CHSS was less than 5 MPa in fewer than 1% of cases [6].

To verify the stability, the RTR-HFP did not apply the PRR calculated in real time if the pressure of the gas in the CHSS was less than or equal to 2 MPa but used the pre-calculated APRR instead. When the initial pressure of the CHSS tank was 0 MPa, the simulation results are shown in Fig. 2.

**2. Safety of RTR-HFP**

In the fueling protocol, fueling is provided to the CHSS and fueling station, and control targets are put in place to prevent the CHSS from being damaged owing to high temperature, high pressure, and excessive mass flow rates, and ensure that no one entering the fueling station is exposed to any risk [19]. Hence, the fueling protocol ensures that the temperature and pressure in the CHSS and the mass flow rate in the fueling line do not exceed the safety limits, and that the fueling system has integrity in functionality [19]. It is imperative to ensure the safety and integrity of the RTR-HFP because it directly uses data measured from the CHSS for fueling control [6]. Table 2 lists the control safety functions included in the RTR-HFP following ISO 19880-1 for safely achieving the control target in the fueling protocol [19].

The control safety functions are divided into basic safety functions and failure diagnosis functions, and are further divided into fueling start control, fueling run control, fueling stop control, and fueling end control. This means that the RTR-HFP has layers of safety-control functions. The RTR-HFP sets and applies the upper limit of the PRR to prevent over-fueling. The upper limit of the PRR was calculated by obtaining the remaining minimum fueling time ($t_{final,\,min}$), which was calculated by dividing the remaining fueling volume by the upper limit of the fueling flow rate (e.g., 60 g/s), and dividing the difference between the maximum supply gas pressure ($P_{ba,\,max}$) and current supply gas pressure ($P_{ba}$) by the minimum fueling time ($t_{final,\,min}$).

**Table 2. RTR-HFP's safety-related functions**

| Types | Functions |
|---|---|
| Basics Safety Function | A-1. Check the upper limit of mass flow rate in the CHSS→Fueling not started if exceeded |
| | A-2. Check pressure rating match between station and CHSS→If match not found, fueling not started |
| | A-3. Comply with the time limit for fueling start→Fueling not started if exceeded |
| | A-4. Set the default upper limit of PRR→Apply upper limit if PRR exceeds it. |
| | A-5. Set the upper limit of PRR according to the fuel remaining time→Apply upper limit if PRR exceeds it. |
| | A-6. Set the upper limit of the control target to 83 °C considering the temperature sensor error |
| | A-7. PRR calculation time limit setting→Shut off if exceeded |
| | A-8. Monitoring the normal communication function→Shut off if abnormal |
| | A-9. Monitor CHSS for exceeding temperature and pressure limits→Shut off if exceeded |
| | A-10. Monitor whether the supply gas pressure exceeds the allowable range→Shut off if exceeded |
| | A-11. Response of abort signal from CHSS→Shut off when received |
| | A-12. Securing the functional safety of the control system (described separately below) |
| Failure Diagnosis Function | B-1. Check capacity of CHSS for abnormalities→Shut off if abnormalities are found |
| | B-2. Check for abnormalities in the mass flow meter→Shut off if abnormalities are found |
| | B-3. Check pressure measuring device fault in CHSS→Shut off in case of failure |
| | B-4. CHSS Check temperature measuring device fault→Shut off in case of failure |

$$t_{final,\,min} = \frac{m_{final} - \left(m_0 + \int_0^t \dot{m}dt\right)}{\dot{m}_{uplim}} = \frac{\rho_{lim} \times V_{tank} - \left(m_0 + \int_0^t \dot{m}dt\right)}{\dot{m}_{uplim}} \quad (18)$$

$$PRR_{uplim} = \frac{P_{ba,\,max} - P_{ba}}{t_{final,\,min}} \quad (19)$$

Applying the upper limit of the PRR, calculated as above, to fueling control would increase its efficiency because it can reasonably pace the fueling speed when it becomes difficult to increase the supply gas pressure indefinitely.

The HFP intended to control safety must not only ensure safety performance in the logic to prevent damage to the CHSS owing to high temperature, high pressure, and excessive mass flow rates, but also maintain integrity of the control system. In addition, since the RTR-HFP uses thermodynamic variables collected in real time to control safety in the fueling process, robustness must be ensured for any error in the sensors that measure the variables. Fig. 3 shows process control results when $T_{tk}$ was measured 5 °C lower than the actual value, and $P_{tk}$ was measured 1.5 MPa higher than the actual value. Even with poor fueling conditions, such as $P_{tk}(0)$=0.5 MPa, $T_{amb}$=50 °C, and $T_{ba}$=−17.5 °C, the temperature in the CHSS did not exceed 85 °C. Moreover, Fig. 4 shows process control results under the same fueling conditions as Fig. 3, but when $T_{ba}$ and $T_{tk}$ were measured 3 °C lower than the actual values, and $P_{ba}$ and $P_{tk}$ were measured 1.5 MPa higher than the actual values. In both cases, the temperature of the CHSS did not exceed 85 °C. ISO 19880-1

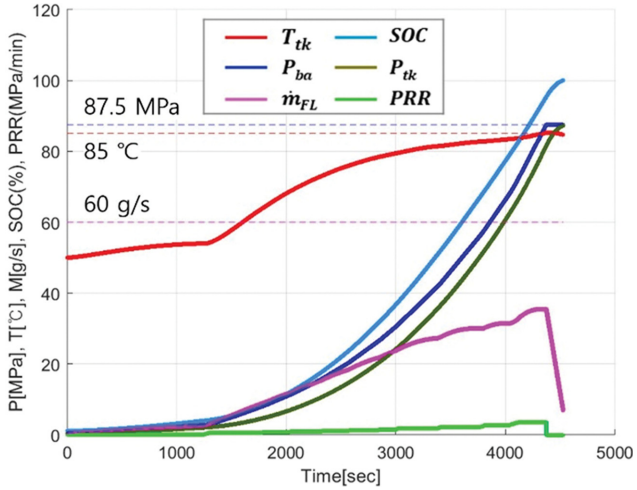


**Fig. 3. When $T_{tk}$ sensor has −5 °C deviation and $P_{tk}$ sensor has error of 1.5 MPa; nominal working pressure of 70 MPa, $V_{tk}$ of 1,740 L (ten 174 L tanks), initial tank pressure of 0.5 MPa, $T_{amb}$ of 50 °C, and $T_{ba}$ of −17.5 °C.**

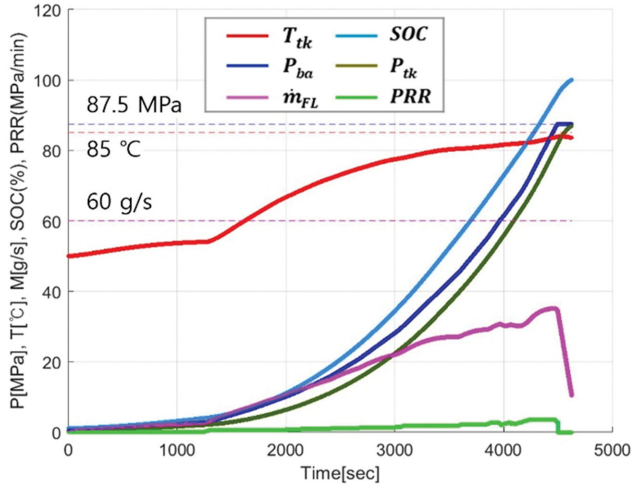


**Fig. 4. When $T_{tk}$ and $T_{ba}$ sensors have −3 °C error and $P_{tk}$ and $P_{ba}$ sensor has error of 1.5 MPa; nominal working pressure of 70 MPa, $V_{tk}$ of 1,740 L (ten 174 L tanks), initial tank pressure of 0.5 MPa, $T_{amb}$ of 50 °C, and $T_{ba}$ of −17.5 °C.**

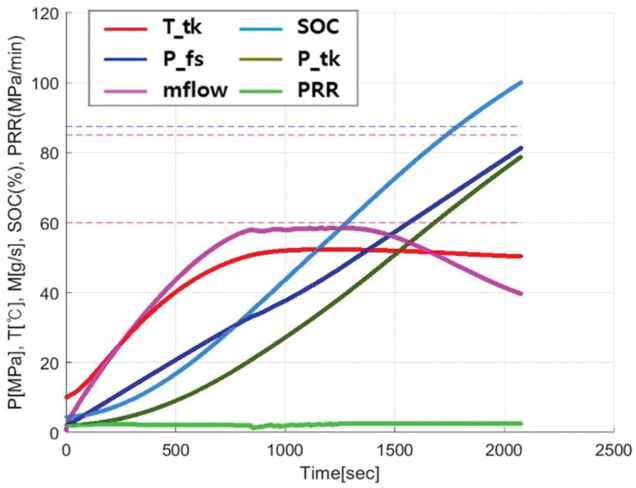


**Fig. 5. 100 kg tanks are fueled by RTR-HFP; nominal working pressure of 70 MPa, $V_{tk}$ of 2,490 L (ten 249 L tanks), initial tank pressure of 2 MPa, $T_{amb}$ of 10 °C, and $T_{ba}$of −33 °C.**

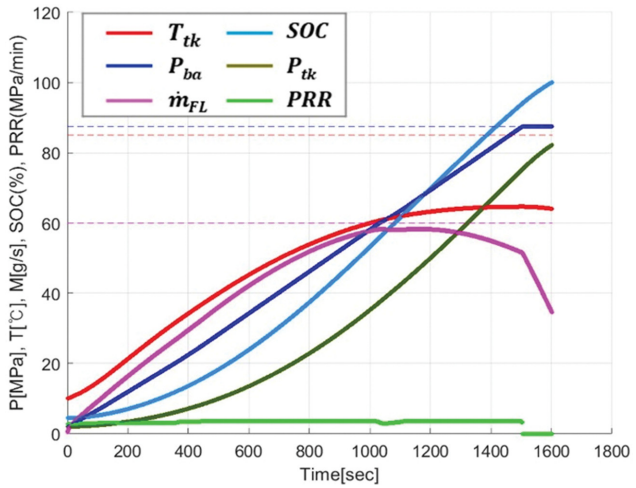


**Fig. 6. RTR-HFP fueling is tested with the upper limit on hydrogen flow rate, $\dot{m}_{uplim}$=60 g/s; nominal working pressure of 70 MPa, $V_{tk}$ of 1,740 L (ten 174 L tanks), initial tank pressure of 2 MPa, $T_{amb}$ of 10 °C, and $T_{ba}$ of −33 °C.**

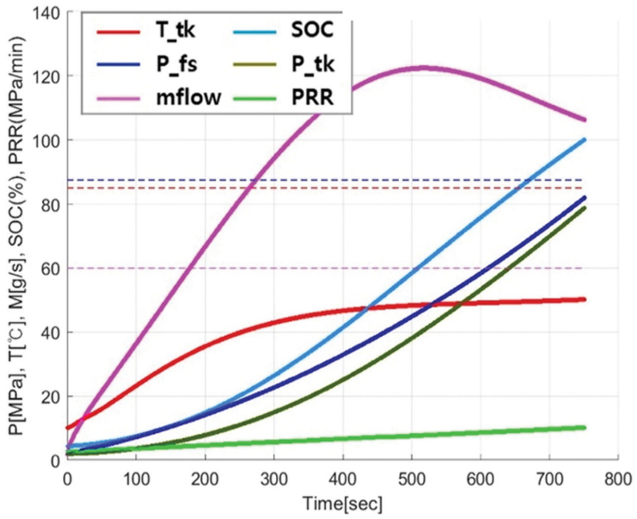


**Fig. 7. RTR-HFP fueling is tested with the upper limit on hydrogen flow rate, $\dot{m}_{uplim}$=240 g/s; nominal working pressure of 70 MPa, $V_{tk}$ of 1,740 L (ten 174 L tanks), initial tank pressure of 2 MPa, $T_{amb}$ of 10 °C, and $T_{ba}$of −33 °C.**

defines the margin of error in sensors measuring supply gas temperature and pressure in the fueling station as ±2 °C and ±1% (±1.2 MPa), respectively. Assuming that the margin of error for the temperature and pressure sensors in the CHSS is equal, the performance of the RTR-HFP despite errors in the temperature and pressure sensors would still be robust.

### 3. Versatility of RTR-HFP

The RTR-HFP gains many advantages by applying the real-time responding MPC technique. In particular, it can control the process for heavy-duty applications and perform high-flow fueling, which is required for heavy-duty applications. Fig. 5 shows the process control results for the 100 kg CHSS. $T_{tk}$ did not increase because not much heat was released through the tank wall. $\dot{m}_{FL}$ was well controlled without exceeding $\dot{m}_{uplim}$ (60 g/s). Meanwhile, Figs. 6 and 7 show the process control results when $\dot{m}_{uplim}$ was set to 60 g/s and 120 g/s, respectively. Under the same conditions, the fueling time decreased by 43%, from 28 to 16 min.

## FUNCTIONAL SAFETY FOR RTR-HFP

Regardless of how perfect the logic of the fueling protocol is, safety is not guaranteed if the control system cannot ensure integrity. In this regard, ISO 19880-1: 2020 states that "the required reliability, or SIL, of safety measures intended to prevent a hazardous situation in case of a failure of the dispensing system control system hardware or software with regards to pressure and gas temperature, should be determined through risk assessment [19]."

HAZOP and layer of protection analysis (LOPA) were used as risk assessment methods to ensure the integrity of the dispensing control system. HAZOP is a technique to identify risk factors. In contrast, LOPA evaluates the effectiveness of independent protection layers (IPL), which reduces the accident frequency or intensity [20]. The specific methods and procedures for identifying risk factors and conducting safety integrity level (SIL) verification using these risk assessment methods are specified in IEC 61882, IEC 61508, and IEC 61511.

We conducted a risk assessment to establish safety criteria for RTR-HFP. Assuming that the draft RTR-HFP was included in a hypothetical dispensing control system, we conducted HAZOP on the control system and obtained the deviation of parameters, causes of the deviation, frequency of the deviation, and their consequences (see Table 3). The failures of sensors and control valves correspond to the failures of basic process control system (BPCS), and these frequencies are set as 0.1 in the Center for Chemical Process Safety (CCPS) Handbook. Based on the initiating cause and initiating event frequency (IEF) shown in Table 3, we conducted LOPA and obtained target mitigated event likelihood (TMEL), IPLs, and the average probability of failure on demand (PFDavg) shown in Table 4.

**Table 3. HAZOP study of RTR-HFP**

| | Deviations | Causes | IEF (/yr) | Consequences |
|---|---|---|---|---|
| 1 | High Temp. | BUF of TS in CHSS of 1 set of tank | 1.00E-01 | CHSS explosion by overheat |
| 2 | High Temp. | HF of TS in CHSS of 1 set of tank | 1.00E-01 | CHSS explosion by overheat |
| 3 | High Temp. | BUF of TS in CHSS of 2 sets of tank | 1.00E-01 | CHSS explosion by overheat |
| 4 | High Temp. | HF of TS in CHSS of 2 sets of tank | 1.00E-01 | CHSS explosion by overheat |
| 5 | High Temp. | BUF of the ambient TS in H2 station | 1.00E-01 | CHSS explosion by overheat |
| 6 | High Temp. | HF of the ambient TS in H2 station | 1.00E-01 | CHSS explosion by overheat |
| 7 | High Temp. | BUF of the supply gas TS in H2 station | 1.00E-01 | CHSS explosion by overheat |
| 8 | High Temp. | HF of the supply gas TS in H2 station | 1.00E-01 | CHSS explosion by overheat |
| 9 | High Temp. | FCV malfunction open in H2 station | 1.00E-01 | CHSS explosion by overheat |
| 10 | High Temp. | One of the CHSS tanks is closed | 1.00E-01 | CHSS explosion by overheat |
| 11 | High Press. | BUF of the supply gas PS(g) in H2 station | 1.00E-01 | CHSS explosion by over pressure |
| 12 | High Press. | HF of the supply gas PS in H2 station | 1.00E-01 | CHSS explosion by over pressure |
| 13 | High Press. | BUF of the CHSS PS | 1.00E-01 | CHSS explosion by overheat |
| 14 | High Press. | HF of the CHSS PS | 1.00E-01 | CHSS explosion by overheat |

BUF: Burn up failure, TS: Temperature sensor, FCV: Flow control valve of station, SOV: Shut off valve, HHS: High high signal, HF: Holding failure, PS: Pressure sensor, IEF: Initiating Event Frequency

**Table 4. LOPA of RTR-HFP**

| | Deviations | TMEL (/yr) | IPLs | PFD | Required $PFD_{avg}$ | Target SIL | SIFs |
|---|---|---|---|---|---|---|---|
| 1 | High Temp. | 1.00E-05 | Protocol: Close FCV by BUF signal from TS | 1.00E-01 | 1.00E-03 | 3 | SIF#1: Install 1 additional TS, Shut off SOV by HHS from TS(1oo2) |
| 2 | High Temp. | 1.00E-05 | Protocol: Check CHSS temp. error, close FCV | 1.00E-01 | 1.00E-03 | 3 | SIF#1: Install 1 additional TS, Shut off SOV by HHS from TS(1oo2) |
| 3 | High Temp. | 1.00E-05 | Protocol: Close FCV by BUF signal from TS | 1.00E-01 | 1.00E-03 | 3 | SIF#2: Shut off SOV by HHS from TS(1oo2) |
| 4 | High Temp. | 1.00E-05 | Protocol: Check CHSS temp. error, close FCV | 1.00E-01 | 1.00E-03 | 3 | SIF#2: Shut off SOV by HHS from TS(1oo2) |
| 5 | High Temp. | 1.00E-05 | Alarm: Backup and differential alarm | 1.00E-01 | 1.00E-02 | 2 | SIF#2: Shut off SOV by HHS from TS(1oo2) |
| | | | Procedure: Periodic check | 1.00E-01 | | | |
| 6 | High Temp. | 1.00E-05 | Alarm: Backup and differential alarm | 1.00E-01 | 1.00E-02 | 2 | SIF#2: Shut off SOV by HHS from TS(1oo2) |
| | | | Procedure: Periodic check | 1.00E-01 | | | |
| 7 | High Temp. | 1.00E-05 | Alarm: Backup and differential alarm | 1.00E-01 | 1.00E-02 | 2 | SIF#2: Shut off SOV by HHS from TS(1oo2) |
| | | | Procedure: Periodic check | 1.00E-01 | | | |
| 8 | High Temp. | 1.00E-05 | Alarm: Backup and differential alarm | 1.00E-01 | 1.00E-02 | 2 | SIF#2: Shut off SOV by HHS from TS(1oo2) |
| | | | Procedure: Periodic check | 1.00E-01 | | | |
| 9 | High Temp. | 1.00E-05 | Protocol: Close FCV when CHSS temp. greater than 85 °C | 1.00E-01 | 1.00E-03 | 3 | SIF#2: Shut off SOV by HHS from TS(1oo2) |
| 10 | High Temp. | 1.00E-05 | Protocol: Check CHSS volume error, close FCV | 1.00E-01 | 1.00E-03 | 3 | SIF#2: Shut off SOV by HHS from TS(1oo2) |
| 11 | High Press. | 1.00E-05 | Protocol: Operation of press. upper limit | 1.00E-01 | 1.00E+00 | −1 | No SIF |
| | | | Mechanical PRD: Operation of PSV on CHSS | 1.00E-02 | | | |
| | | | Procedure: Periodic check | 1.00E-01 | | | |
| 12 | High Press. | 1.00E-05 | Protocol: Operation of press. upper limit | 1.00E-01 | 1.00E+00 | −1 | No SIF |
| | | | Mechanical PRD: Operation of PSV on CHSS | 1.00E-02 | | | |
| | | | Procedure: Periodic check | 1.00E-01 | | | |
| 13 | High Press. | 1.00E-05 | Protocol: Close FCV by BUF from CHSS PS | 1.00E-01 | 1.00E-03 | 3 | SIF#2: Shut off SOV by HHS from TS(1oo2) |
| 14 | High Press. | 1.00E-05 | Protocol: Check PS error by comparison, close FCV | 1.00E-01 | 1.00E-03 | 3 | SIF#2: Shut off SOV by HHS from TS(1oo2) |

BUF: Burn up failure, TS: Temperature sensor, FCV: Flow control valve of station, SOV: Shut off valve, HHS: High high signal, HF: Holding failure, PS: Pressure sensor

We also considered the safety instrumented function (SIF) to meet the SIL target.

Tables 3 and 4 summarize the 14 factors that have a material effect on the temperature and pressure in the CHSS among a total of 21 factors in the risk assessment. Most IPLs were confirmed to ensure safety when two SIFs were introduced, as reflected in the RTR-HFP draft. Fig. 8 provides a conceptual diagram of the dispensing control system, which incorporates these two SIFs, while

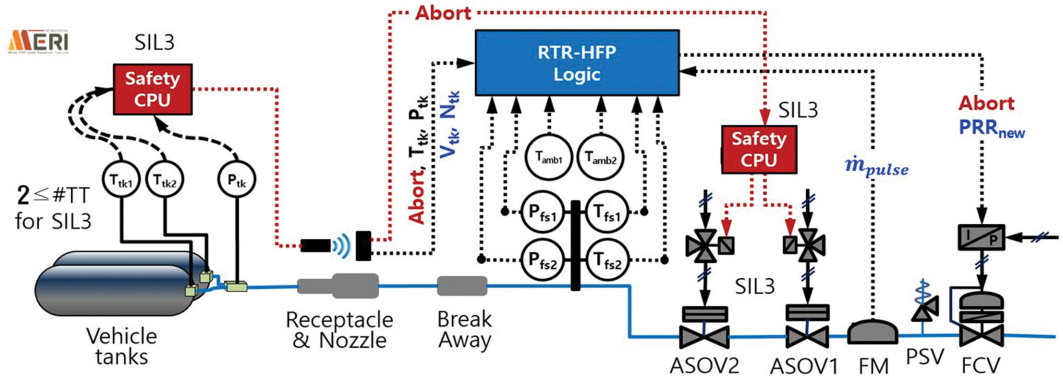


**Fig. 8. Conceptual diagram of fueling control system to secure SIL.**

**Table 5. Functional safety of fueling control system**

| Types | Functional safety |
|---|---|
| CHSS | • Install at least two temperature sensors<br>• Install Safety CPU (Fail safe) for signal processing<br>• Install the safety valve in each tank<br>• Attach RTR-HFP applicable recognition mark (government issued) to the receptacle |
| Fueling system | • Install Safety CPU for emergency shut-off valve operation<br>• Establish an independent communication line connecting safety CPU of CHSS to safety CPU of fueling system<br>• Redundancy of emergency shut-off valves operated by the fueling system's safety CPU (installation of two or more)<br>• Redundancy of the supply gas temperature/pressure and ambient air temperature measuring device (installation of two or more) |

Table 5 shows a list of functional safety measures.

In detail, for LOPA, TMEL of 1E-5/yr was used as the risk tolerance for one fatality, and PFDavg of IPL was referred to IPL Table in CCPS Handbook. For example, for the scenario 1 having the IEF of 1E-1/yr, the intermediate event likelihood (IEL) is calculated by

$$IEL=IEF\times IPL=1E\text{-}1/yr\times 1E\text{-}1=1E\text{-}2/yr.$$

Furthermore, the required PFDavg is calculated by

$$\text{Required PFDavg}=TMEL/IEL=(1E\text{-}5/yr)\div(1E\text{-}2/yr)=1E\text{-}3$$

## CONCLUSIONS

We improved the real-time responding HFP (RTR-HFP), which was suggested in our previous study, in terms of operability, stability, safety, and performance. Traditional HFPs, TB-HFP and MC-HFP control the fueling process based on simulation of the thermodynamic model and use the PRR to control the fueling process. To some extent, the RTR-HFP also utilizes the TB-HFP lookup table from traditional fueling protocols and thermodynamic data in the CHSS. It would be fair to say that the traditional fueling protocols and RTR-HFP belong to the same species.

RTR-HFP shows the following benefits from applying a real-time response technique. First, the proposed protocol can improve the fueling time efficiency while guaranteeing safety. Second, it can respond to all types of changes in the fueling conditions, including the supply gas temperature, outdoor air temperature, and initial CHSS pressure. Third, it can be applied to various vehicles, from small personal vehicles to commercial large-mobility vehicles, in a versatile manner. Fourth, it can immediately respond to a new problem, meaning that it is easy to change the constraints if there is a problem with applicability, stability, and safety. Fifth, it is simpler to document RTR-HFPs for scalability and applicability.

Because RTR-HFP uses data collected in real time for control, the reliability of the data and functional safety in the control system must be ensured. To this end, we conducted risk assessment and identified effective response options.

## ACKNOWLEDGEMENTS

This study was part of, and funded by, the Ministry of Trade, Industry, and Energy (MOTIE) and the Korea Institute of Energy Technology Evaluation and Planning (KETEP) Energy International Joint Research Project (No. 20203010040010).

## NOMENCLATURE

A : area of fueling line cross section [$m^2$]
$C_v$ : specific heat capacity at constant volume [kJ/kg·K]
d : inner diameter of fueling [m]
E : total energy [kJ/kg]
h : static enthalpy [kJ/kg]
K : pressure drop coefficient of fueling line [$m^{-4}$]
m : mass of compressed hydrogen [kg]
$\dot{m}$ : mass flow rate of compressed hydrogen [kg/s]

N : number of tanks
P : pressure [MPa]
PRR : pressure ramp rate [MPa/s]
Q : heat transferred [kJ]
R : universal gas constant (8.314 472) [J/mol·K]
T : temperature [K]
$\Delta T_s$ : sampling time [s]
v : velocity of flowing hydrogen [m/s]
V : volume of CHSS tank [$m^3$]
Z : compressibility factor
$\rho$ : gas density [$kg/m^3$]

**Subscript**

ba : break away
final : fueling end time
FL : fueling line
hot : hot case
max : maximum
min : minimum
ref : reference state
sg : stagnation enthalpy
st : station
ti : tank inlet
tk : vehicle tank
uplim : upper limit

## REFERENCES


1. J. Schneider, G. Meadows, S. R. Mathison, M. J. Veenstra, J. Shim, R. Immel, M. Wistoft-Ibsen, S. Quong, M. Greisel, T. McGuire and P. Potzel, *SAE Int. J. Altern. Powertrains*, **3**, 2 (2014).
2. F. Olmos and V. I. Manousiouthakis, *Int. J. Hydrogen Energy*, **38**, 8 (2013).
3. K. Handa, S. Yamaguchi, K. Minowa and S. Mathison, *SAE Int. J. Altern. Powertrains*, **6**, 2 (2017).
4. S. Pregassame, F. Barth, L. Allidieres and K. Barral, 16th World Hydrog. Energy Conf. (2006).
5. Society of Automotive Engineers. SAE J2601: Fueling Protocols for Light Duty Gaseous Hydrogen Surface Vehicles. SAE International (2016).
6. S. Mathison, How Advanced Hydrogen Fueling Protocols can Improve Fueling Performance & H2 Station Design (2020).
7. S. Mathison, K. Handa, T. McGuire, T. Brown, T. Goldstein and M. Johnston, *SAE Int. J. Altern. Powertrains*, **4**, 1 (2015).
8. R. Harty, S. Mathison and N. Gupta. Proc. Natl. Hydrog. Assoc. Conf. (2010).
9. C. K. Chae, B. H. Park, Y. S. Huh, S. K. Kang, S. Y. Kang and H. N. Kim, *Int. J. Hydrogen Energy*, **45**, 30 (2020).
10. B. Thomas, B. Frederic, B. Thomas, R. Baptiste and D. Clemence, D5.1 Validation of a new approach for fast filling of hydrogen tanks, HyTransfer (2017).
11. K. Handa and S. Yamaguchi, *Int. J. Automot. Eng.*, **9**, 4 (2018).
12. S. Yamaguchi, Y. Fujita and K. Handa, 31st Int. Electr. Veh. Symp. Exhib. EVS (2018).
13. E. D. Rothuizen, *Hydrogen fuelling stations: A thermodynamic analysis of fuelling hydrogen vehicles for personal transportation*, Ph.D. Thesis. Technical University of Denmark (2013).
14. M. Monde, Y. Mitsutake, P. L. l. Woodfield and S. Maruyama, *Heat Transf. - Asian Res.* **36**, 1 (2007).
15. E. W. Lemmon, M. L. Huber and J. W. Leachman, *J. Res. Natl. Inst. Stand. Technol.*, **113**, 6 (2008).
16. Y. A. Çengel, M. A. Boles and M. Kanoglu, *Thermodynamics: An engineering approach*, McGraw-Hill Education (2018).
17. Y. A. Çengel and J. M. Cimbala, *Fluid mechanics: Fundamentals and applications*, 4th ed. McGraw-Hill Education (2018).
18. V. Molkov, M. Dadashzadeh and D. Makarov, *Int. J. Hydrogen Energy*, **44**, 8 (2019).
19. The International Organization for Standardization. ISO/TS 19880-1 (2016): Gaseous hydrogen - Fuelling - Part 1: General requirements. (2016).
20. J. Ahn, Y. Noh, T. Joung, Y. Lim, J. Kim, Y. Seo and D. Chang, *Int. J. Hydrogen Energy*, **44**, 5 (2019).